Stability of Climate Networks with Time

Y. Berezin, A. Gozolchiani, and S. Havlin
*Minerva Center and Department of Physics, Bar Ilan University, Ramat Gan, Israel.**
(Dated: September 27, 2011)

We construct and analyze climate networks based on daily satellite measurements of temperatures and geopotential heights. We show that these networks are stable during time and are similar over different altitudes. Each link in our network is stable with typical 15% variability. The entire hierarchy of links is about 80% consistent during time. We show that about half of this stability is due to the spatial 2D embedding of the network, and half is due to physical coupling mechanisms. The network stability of equatorial regions is found to be lower compared to the stability of a typical network in non–equatorial regions.

PACS numbers: 05.40.-a,89.75.-k,89.60.Gg

I. INTRODUCTION

During the past decade, methods from network theory have been applied to describe complex systems that are composed of many interacting components (see e.g. [1–26]). While in some cases the representation of such systems as a network is obvious and the nodes and links are identified directly (e.g. cables connecting computers in a computer network) [2], in many real world networks such as biological systems [4], neural networks [26], climate networks [27–35] and others, the identification of links is not direct and it is based on statistical analysis of the similarity of the dynamics of nodes [36].

In recent years it was suggested that climate fields such as temperature and geopotential height at a certain pressure level can be represented as a climate network where the nodes are geographical sites and the links are the information flow between these sites (nodes). Although the dynamics within a single node is unpredictable and chaotic, yet the dynamic of one node may be coupled to the dynamics of other nodes and could be observed. The correlations between the dynamics in two different nodes is represented in our network as a link between them. Since we deal with climatological data, the correlations (Sec. II B) might be with a time-delay. Therefore, each link is quantified by two parameters; a strength value which quantifies the intensity of the cross correlations, and a time delay value which quantifies the delay in the data flow between the two nodes.

II. THE CLIMATE NETWORK

A. Data

We analyze data obtained from a reanalysis project [37]. The records consist of the reanalysis air temperature field and the geopotential height field, for the 1000hPa, 925hPa, 850hPa, 700hPa, 500hPa and 300hPa isobars. We use daily values between the years 1948-2006. The data is arranged on a world-wide grid with a resolution of $5^\circ \times 5^\circ$. We divide the globe into 9 zones (see Fig. 1), in order to identify different network dynamics specific to different zones.

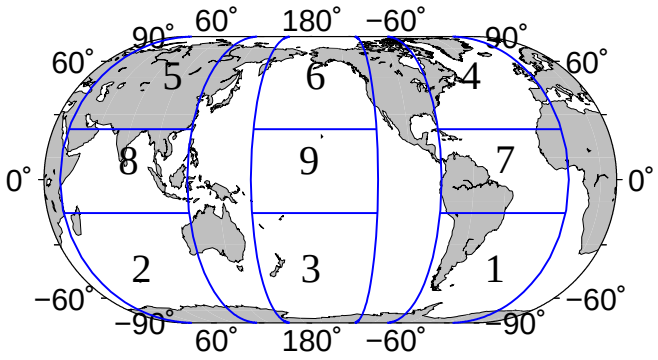

FIG. 1: (color online). The geographical locations of the 9 separate zones, on which we base our network analysis.

B. The network construction method

We analyze daily climatological records (temperature/pressure) taken from a grid in various geographical zones (Fig. 1). To avoid the trivial effect of seasonal trends we subtract from the records of each day the yearly average value of that day. Specifically, we take the climatological signal (temperature/pressure) of a given site in the grid to be $\widetilde{S}^y(d)$, where y is the year and d is the day (ranging from 1 to 365) of that year. The new signal will be $S^y(d) = \widetilde{S}^y(d) - \frac{1}{N}\sum_y \widetilde{S}^y(d)$, where N is the number of years available in the record. For each pair of sites l and r in a specific zone, we compute the absolute value of the cross-covariance function $X^y_{l,r}$ of their local climatological signals such as temperature/pressure in the range of time delays $\tau \in [-\tau_{max}, \tau_{max}]$ integrated

*Electronic address: bereziny@google.com

over a specific year (y) (see Fig. 2). Using the cross-covariance function $X^y_{l,r}$ we define the strength of the link to be $W^y_{l,r} = (MAX(X^y_{l,r}) - < X^y_{l,r} >)/STD(X^y_{l,r})$, where $< \ldots >$, MAX and STD are the mean value, maximal value and the standard deviation of $X^y_{l,r}$ in the range of τ, respectively. The matrix $W^y_{l,r}$ represents the *weighted adjacency matrix* of the network at year y. The time shift at which $X^y_{l,r}$ is maximal is defined as the link time delay, and denoted as $T^y_{l,r}$.

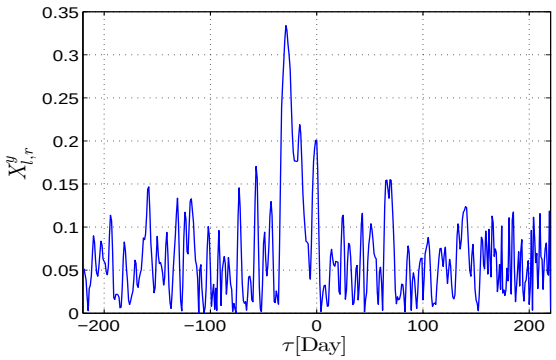

FIG. 2: A typical cross-covariance function between two sites, representing the level of correlation within a time lag ranging from $-\tau_{max}$ to $+\tau_{max}$ where $\tau_{max} = 220$. In the current example $W^y_{l,r} = \frac{0.3-0.05}{0.05} = 5$, $T^y_{l,r} = -15$.

III. RESULTS

A. Stability of single links

First we focus on the behavior of single links. We analyze the yearly variations of the link strength $W^y_{l,r}$. We find that a typical link maintains its strength $W_{l,r}$ during the years with typically small fluctuations of 15%. This stability in the strength of the links behavior is valid for links across long and short distances (see Fig. 3). In Fig. 4 we show the distribution of the relative standard deviation of all links in two networks (a) the network located at Zone 1 (a non–equatorial region) and (b) the network located at Zone 9 (an equatorial region) (see Fig. 1). We observe a significant difference in this distribution between networks located in equatorial regions and networks located in non-equatorial regions. While in networks located in equatorial regions (zones 7-9), the minimum variation is about 0.1 and the maximum is about 0.3, in networks located in non–equatorial regions (zones 1-6), the minimum variation is about 0.05 and the maximum is about 0.25 (see Fig. 4). Therefore the link strengths, $W_{l,r}$, in non–equatorial regions tend to be more stable than the link strengths, $W_{l,r}$, in equatorial regions.

A typical auto-correlation function for climatological records of a specific node decays rapidly as a power low with time [38–43]. Therefore, this stability of the links over many years is surprising and may suggest that we can extract new information from the links between the nodes.

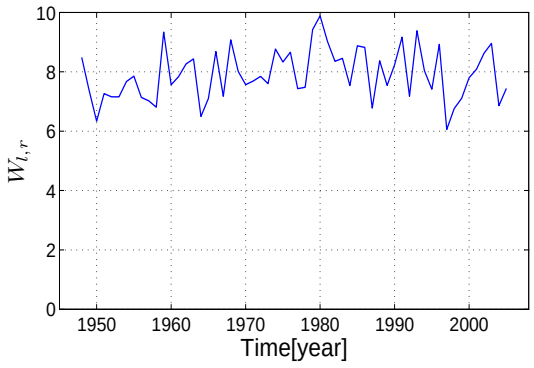

(a) Short distance link ($750Km$)

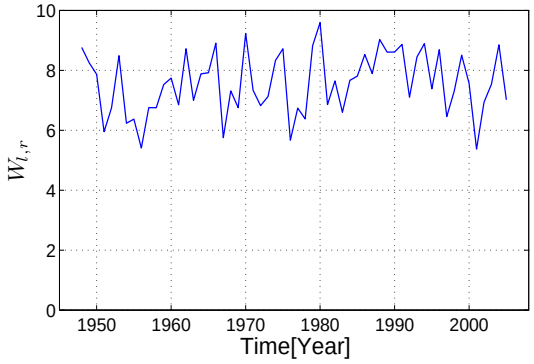

(b) Long distance link ($1500Km$)

FIG. 3: Two examples of typical dynamics of a link strength (W) during the years. In (a) the distance between the two sites is about $750Km$, the average time delay $\overline{T} = 0$ (day) and the variation in the link strength, $STD(W_{l,r})/\overline{W_{l,r}} = 0.1$. In (b) the distance between the two sites is about $1500Km$, the average time delay $\overline{T} = 1$ (day) and the variation in the link strength, $STD(W_{l,r}) = 0.1$.

Analyzing the influence of spatial distances D, between the nodes on the strength W_D of the link leads to the observation of a strong dependence of W_D on D (Fig. 5). Here $W_D \equiv \overline{W}^y_{l,r}$ is the average over all link strengths W at distance D, and over all years, y. It is seen that for $D > 2000$ Km, W_D reaches a low and almost constant value. This constant value can be regarded (as will be seen in Sec IV A) as the level of noise. However, we observe a significant difference in this dependence between networks located in equatorial regions and networks located in non-equatorial regions (compare Fig. 5(a) and Fig. 5(b)). In networks located in equatorial regions (zones 7-9), W_D decreases significantly slower with time compared to other regions. This difference mainly appears in networks based on the geopotential height field.

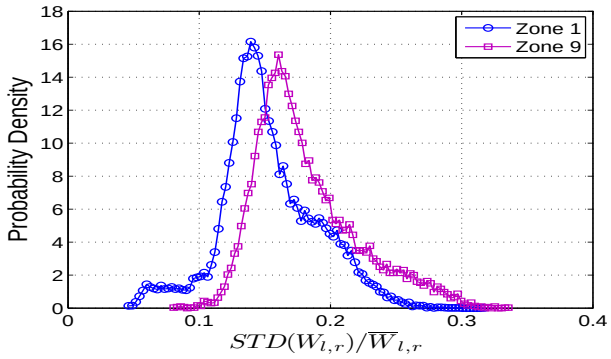

FIG. 4: Distribution of the links variation during time, $STD\,(W)\,/\overline{W}$ in two zones. Zone 1 and Zone 9, both for network based on temperature at 850hPa isobar.

B. Stability of the entire network

In Sec. III A we showed that single links remain relatively stable. In this section we study the stability of the entire hierarchy of links within the climate network. We find the network to be relatively stable over time. This stability of the network may be demonstrated by measuring the similarity between network states in different years. We analyze the similarity by calculating $p(\tau)$ (the Pearson coefficient) between the adjacency matrices of two network states in different years y_1, y_2 as a function of $\tau = y_2 - y_1$. In Fig. 6 (the upper curve) we show the average similarity $\overline{p}(\tau)$ between network structures as a function of the time separation τ. It is seen in Fig. 6(a) that this similarity is indeed high and almost constant, $\overline{p}(\tau) \approx 0.8$. This behavior is consistent for all networks in the non-equatorial regions. For networks in equatorial regions the correlation between the network states in different years, $\overline{p}(\tau)$ is still significantly high but relatively fluctuative. (see Fig. 6(b)).

In Fig. 5 we showed, that there is a strong dependence between the link strength, W and the link distance, D. Links with shorter distances D are therefore more likely to have higher W values, at all times. It is therefore plausible that the high stability of $\overline{p}(\tau) \approx 0.8$ is partially due to this strong dependence. The contribution of the effect of the W–D dependence to this observed stability, on the one hand, and the contribution of physical coupling processes, on the other hand, must be estimated.

We achieve this goal of removing the contribution of the W–D dependence by subtracting from each link strength, $W_{l,r}$ the average strength of the group of links with a similar distance, $\overline{W}_D$. A new, transformed adjacency matrix, $W_{l,r} - \overline{W}_D$, is thus formed, which does not depend on D. Repeating our analysis of calculating $\overline{p}(\tau)$, for the new adjacency matrix, we show in the lower curve of Fig. 6, the stability of this network. Indeed, after removal of the distance effect, the network exhibits lower $\overline{p}(\tau)$ values. However, the stability related to physical coupling processes is still significant [47].

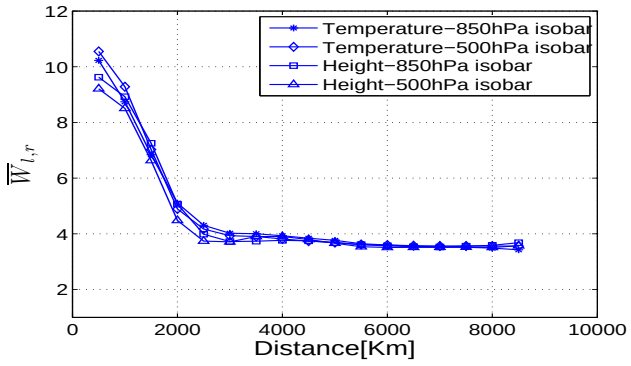

(a) Zone 1

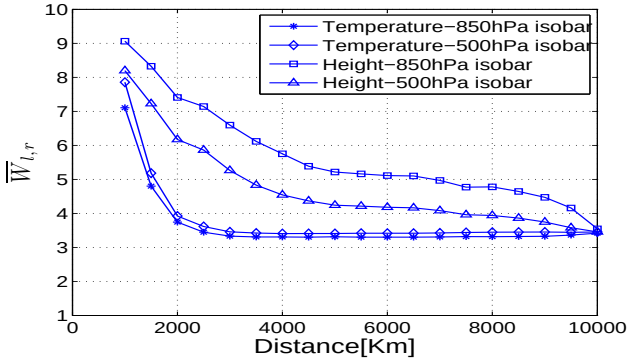

(b) Zone 9

FIG. 5: The dependence of $\overline{W}_{l,r}$ on $D_{l,r}$ in two typical locations, (a) Zone 1 (non–equatorial region). (b) Zone 9 (equatorial region). The four curves describe four networks which are based on geopotential height measurement at 850 and 500hPa isobar and based on temperature measurement at 850 and 500hPa isobar.

It is plausible that some of our network links emerge mainly due to noise and not due to real physical coupling processes. In Sec. IV A we show that this group of false links is characterized by low $W_{l,r}$ values at all times, and that this characterization is sufficient for uniquely identifying this group. In order to identify this group of false links which are due to noise, we define $\overline{W}_{l,r}$ as the average strength of a link $W^y_{l,r}$ over all years. Upon eliminating low weighted links that satisfy $\overline{W}_{l,r} < \theta$ (where θ is a threshold that will be determined later in Sec. IV A) from our network, we observe in the middle curve of Fig. 6 an increase of the network stability. Thus, while the hierarchy of false links rapidly changes in each time step, the hierarchy of significant links (having $\overline{W}_{l,r} > \theta$) is, to a large extent, preserved.

The new $\overline{p}(\tau)$ values, which are calculated after the removal of both the distance effect and the effects of noise, for different regions and fields are summarized in Table I. In contrast to the common $\overline{p}(\tau) = 0.8$ value that was observed for the original network (including the distance and noise effects), after removal of the distance and noise effects we observe lower $\overline{p}(\tau)$ values specific to each zone

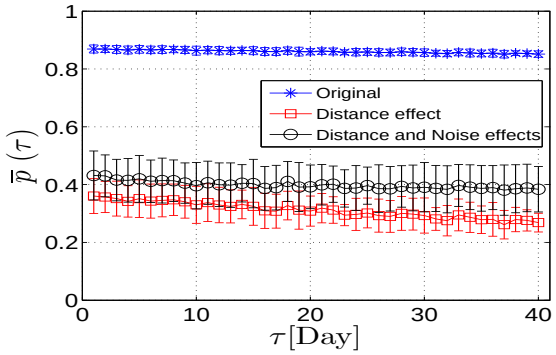

(a) Temp-850hPa, zone1

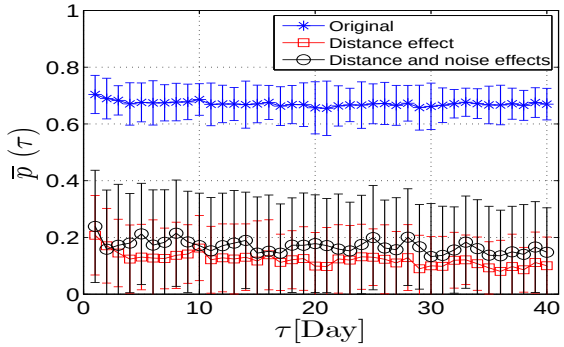

(b) Temp-850hPa, zone9

FIG. 6: The average correlation, $\overline{p}(\tau)$, between network adjacency matrices at different time snapshot, between $\tau = 1$ and $\tau = 40$ *years* apart, for networks based on temperature at 850hPa and located at (a) zone 1, and (b) zone 9. The upper curve in each figure, represents the correlation between the original networks without removing the effects of distance and noise. The lower curve represents $\overline{p}(\tau)$ for a network after removing of the distance effect. The mid curve represents $\overline{p}(\tau)$ for a network after removing both, distance and noise effects.

and climate variable. Still, in general, non equatorial regions exhibit larger stability values than equatorial regions.

It has been shown that during El-Niño times, link strengths, $W^y_{l,r}$, are significantly reduced mainly in equatorial regions [27, 29]. Hence our observation of lower stability in equatorial regions is consistent with the known effect of El-Niño on the climate network.

From Table I we see that removing both the distance effect and the effects of noise reveal that the networks in zone 3, at the southern ocean, exhibit low stability, $\overline{p}(\tau)$ values similar to the equatorial regions. This similarity of the behavior of the network in zone 3 and the behavior of the network in equatorial regions is consistent with the known local oscillations in zone 3 that correlate with ENSO, due to both ocean mechanisms [44] and atmospheric coupling mechanism [45].

zone / climate variable	Temp 850 hPa	Temp 500 hPa	Height 850 hPa	Height 500 hPa
zone 1	0.42 ± 0.08	0.31 ± 0.08	0.48 ± 0.08	0.3 ± 0.1
zone 2	0.4 ± 0.08	0.33 ± 0.08	0.32 ± 0.11	0.3 ± 0.11
zone 3	0.27 ± 0.09	0.21 ± 0.1	0.17 ± 0.13	0.18 ± 0.11
zone 4	0.32 ± 0.08	0.24 ± 0.09	0.45 ± 0.11	0.36 ± 0.1
zone 5	0.42 ± 0.1	0.34 ± 0.1	0.51 ± 0.12	0.42 ± 0.11
zone 6	0.43 ± 0.08	0.41 ± 0.09	0.45 ± 0.08	0.37 ± 0.08
zone 7	0.22 ± 0.11	0.37 ± 0.15	0.37 ± 0.16	0.18 ± 0.17
zone 8	0.33 ± 0.13	0.19 ± 0.14	0.24 ± 0.15	0.14 ± 0.21
zone 9	0.25 ± 0.14	0.2 ± 0.11	0.37 ± 0.14	0.16 ± 0.2

TABLE I: The average correlation values, $\overline{p}(\tau)$, between network adjacency matrices at different time snapshot for networks based on various fields and located at different regions. The values shown are after removing the distance and noise effects.

Based on the high stability values seen in Table I, we conclude that similarity between network states at all times stems from a hierarchy of real physical correlations (links) between different locations, which is preserved in time.

IV. SIMILARITY BETWEEN THE NETWORKS STRUCTURE, IN DIFFERENT ALTITUDES AND DIFFERENT CLIMATE VARIABLES

A further indication that the stability of the network structure reflects a stability of physical coupling processes, is from the finding of similarity between the networks structure in different altitudes, and different climate variables. For example, synchronized heating of two sites at the 850hPa isobar network is likely to also cause synchronized heating of the corresponding sites in the adjacent isobar of 500hPa network by direct heat transport. In the following we show that such a correspondence between networks of different altitudes and climate variables indeed exists.

In Fig. 7 we show the Pearson correlation p^y between the adjacency matrices of the climate networks in the 850hPa isobar and in the 500hPa as a function of time. Similar to Sec. III B the upper curve represents the values of p^y for the original networks, the lower curve is after the removal of the distance effect, and the middle curve is after the removal of both distance and noise effects. As is clearly seen from Fig. 7(a) this correlation is significant, with an average value of $\overline{p^y} \approx 0.6$ and small fluctuation during time. In all non–equatorial (for both temperature and geopotential height) regions we observe similar high $\overline{p^y}$ values. A further observation from Fig. 7(a) is the increase of 10–20% in $\overline{p^y}$ values after the removal of noise.

In contrast, in equatorial regions (see e.g. Fig. 7(b)) we generally observe lower and more fluctuative p^y values. Another difference between non–equatorial and equatorial regions is the smaller effect of the removal of noise

on the p^y.

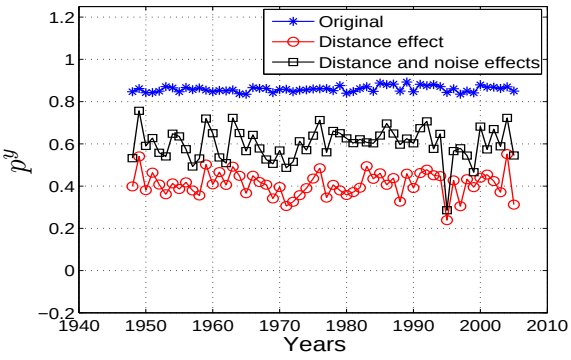

(a) Height-850-500hPa, zone1

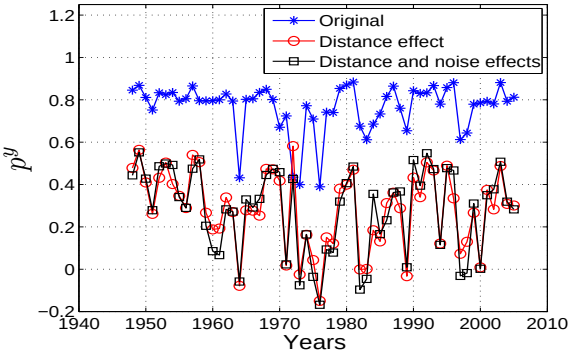

(b) Height-850-500hPa, zone9

FIG. 7: The correlation between two network adjacency matrices at different altitudes, 850hPa isobar and 500hPa isobar in equatorial and non–equatorial regions. (a) Zone 1 (non–equatorial region), and (b) zone 9 (equatorial region). The upper curve in each figure, represents the correlation between the original networks without removing effects of distance and noise. The lower curve represents p^y for the networks after removing the distance effect. The mid curve represents p^y for the networks after removing both, distance and noise effects.

Based on physical considerations it is reasonable that a pair of networks with a larger altitude distance will have a smaller similarity. Indeed such a monotonic decreasing relation is seen in Fig. 8. Each point in the curves of Fig. 8 is an average over different regions, different time snapshots, and different altitudes of the correspondence $\overline{p^y}$. The different curves indicates that this monotonic decrease in the similarity behavior holds both in equatorial and non–equatorial regions and both for temperature and geopotential height networks.

A. Criterion for significant links

Underlying our supporting arguments for the stability of the climate network, there is an assumption. We rely on the existence of a sharp boundary between the properties of links that result due to noise, L_N, and links that

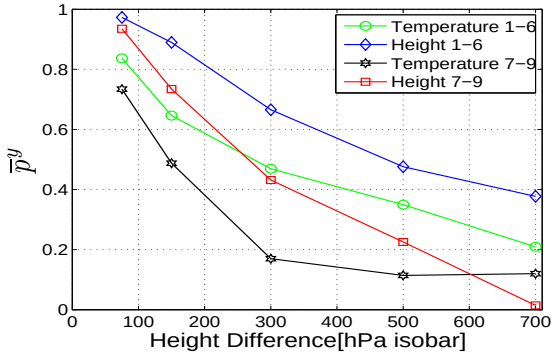

FIG. 8: Average correlations between pairs of networks with different altitude distances. The four curves describe two networks which are located in non–equatorial regions (zones 1–6) and based on geopotential height or based on temperature and two networks which are located in equatorial regions (zones 7–9) and based on geopotential height or based on temperature measurements.

result due to real physical dependence, L_p. The set of all links is $L = L_N \cup L_p$. In this section we will show that such a boundary indeed exists, with respect to two link properties: **(a)** the average over all years of the link strength , $\overline{W}_{l,r}$ and **(b)** the variability over time of the time delays of links $STD(T_{l,r})$. We will later show that using both quantities in order to identify the set of real links L_p converges to almost the same set of links.

Our anchor for comparison between the derived L_p and L_N is the distributions of **(a)** $\overline{W}_{l,r}$ and **(b)** $STD(T_{l,r})$ for networks based on shuffled data. The shuffling scheme is aimed at preserving all the statistical quantities of the data, such as the distribution of values, and their autocorrelation properties, but omitting the physical dependence between different nodes (different geographical locations). The network properties in such a case are only due to the statistical quantities and therefore are similar in their properties to false links. To achieve this shuffling goal, we choose for each node a random sequence of y in S_d^y (the order of the days, d is preserved) [48]. Thereafter, the entire construction of the network, based on correlations of the shuffled records, is performed. The adjacency matrix of the network based on shuffled data is denoted as $w_{l,r}$. The time delay matrix of the network based on shuffled data is denoted as $t_{l,r}$.

(a) Average link strength. In Fig. 9 we compare the probability density function (PDF) of $\overline{W}_{l,r}$ and $\overline{w}_{l,r}$. As clearly seen from these figures, the range of possible $\overline{w}_{l,r}$ is extended only over a limited range of values, $\overline{w}_{l,r} \in [3,4]$. Higher values that exist in the PDF for $\overline{W}_{l,r}$ are missing from the PDF of the shuffled data, and therefore are not likely to occur by chance. The cumulative distribution function (CDF) of $\overline{w}_{l,r}$ (see insets of Fig. 9) can be regarded as an estimate for the likelihood of a $\overline{W}_{l,r}$ value to arise by real physical dependence. The

98% likelihood level is shaded in the inset of Fig. 9(a), having $\overline{W}_{l,r} \geq 4$ for off-equatorial regions, and in the inset of Fig. 9(b), $\overline{W}_{l,r} \geq 3.6$ for equatorial regions.

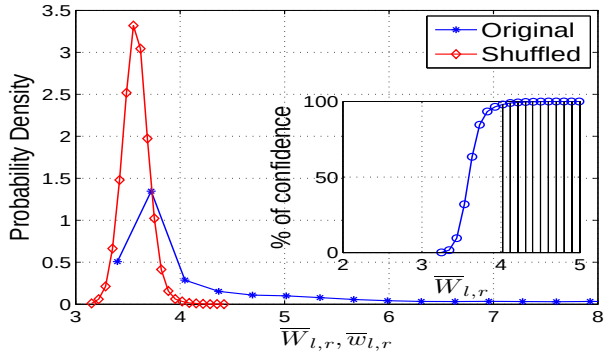

(a) Temp-850hPa, zone1

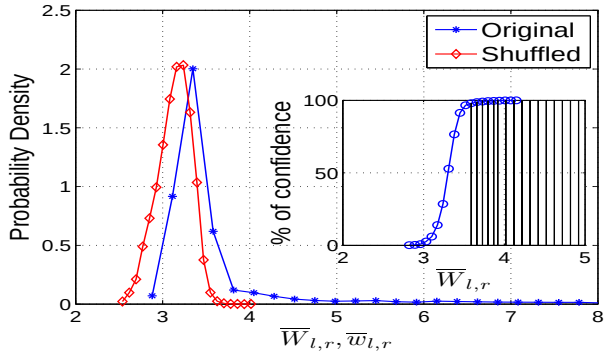

(b) Temp-850hPa, zone9

FIG. 9: The distribution of $\overline{W}_{l,r}$ and $\overline{w}_{l,r}$ in equatorial and non–equatorial regions for networks based on temperature measurements at 850hPa isobar. (a) Zone 1 (non–equatorial region), and (b) zone 9 (equatorial region).

(b) Variation of the time delay. High variability during different years of the time delays of links $STD(T_{l,r})$, is also a signature of artificial (random) behavior [49]. Therefore it serves as another good separator between L_p and L_N. In Fig. 10 we show the probability density function (PDF) of $STD(T_{l,r})$ and $STD(t_{l,r})$. As clearly seen from these figures, the range of possible $STD(t_{l,r})$ is extended over a limited range of values, $STD(t_{l,r}) \in [75, 150]$. Lower values that exist in the PDF of $STD(T_{l,r})$ are missing from the PDF of the shuffled data, and therefore are not likely to arise by chance. The cumulative distribution function (CDF) of $STD(t_{l,r})$ (see inset of Fig. 10) can be regarded as an estimate for the likelihood of a $STD(T_{l,r})$ value to occur by real physical dependence. The 98% likelihood level is shaded in the inset of Fig. 10, having $STD(T_{l,r}) \leq 75$ for off-equatorial regions, and $STD(T_{l,r}) \leq 80$ for equatorial regions.

Both $\overline{W}_{l,r}$ and $STD(T_{l,r})$ can be used for determining a boundary between L_P and L_N. Convergence to similar L_P and L_N in both criterions can be considered as

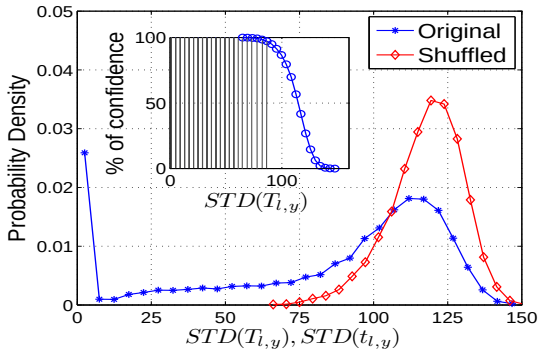

(a) Temp-850hPa, zone1

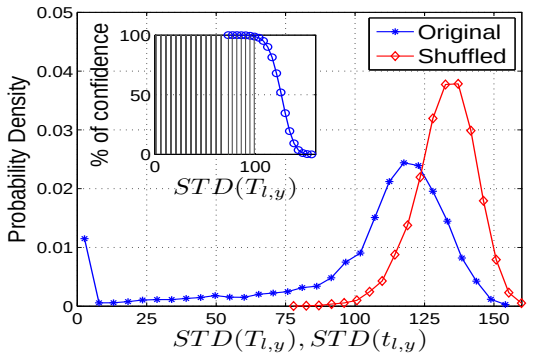

(b) Temp-850hPa, zone9

FIG. 10: The distribution of $STD(T_{l,r})$ and $STD(t_{l,r})$ in equatorial and non–equatorial regions for networks base on temperature measurements at 850hPa isobar. (a) Zone 1 (non–equatorial region), and (b) zone 9 (equatorial region).

a confirmation that either of these criterions indeed efficiently distinct between links that emerge merely due to noise and real links. In Fig. 11 we show a two dimensional PDF of $\overline{W}_{l,r}$ and $STD(T_{l,r})$. A large fraction of the links evidently have both low values of $\overline{W}_{l,r}$ and high values of $STD(T_{l,r})$, which is a typical behavior of links that emerge from random behavior. This set of links is realized as a sharp local maximum of the PDF in the region $\overline{W}_{l,r} \in [3, 4.5], STD(T_{l,r}) \in [75, 150]$ (See Figs. 9 and 10). Within this region, $\overline{W}_{l,r}$ and $STD(T_{l,r})$ are not correlated, since the fluctuations are random in both axes. Outside this region the mutual local maximum of the PDF in both axis are correlated, i.e. larger values of $\overline{W}_{l,r}$ are paired with lower values of $STD(T_{l,r})$. The crossover between the two regimes occurs around $\left(\overline{W}_{l,r}, STD\left(T_{l,r}\right)\right) = (4.5, 75)$. This qualitative behavior is consistent at all regions (1–9), but the crossover point is a bit different for non–equatorial regions (around $(4.0, 75)$).

A further indication that the boundary between L_p and L_N is within the region $\overline{W}_{l,r} \in [3.5, 4.5]$ is the increased sensitivity of the stability measure $\overline{p}(\tau; \theta)$ to the removal of noise within this region. Here we indicate explicitly the

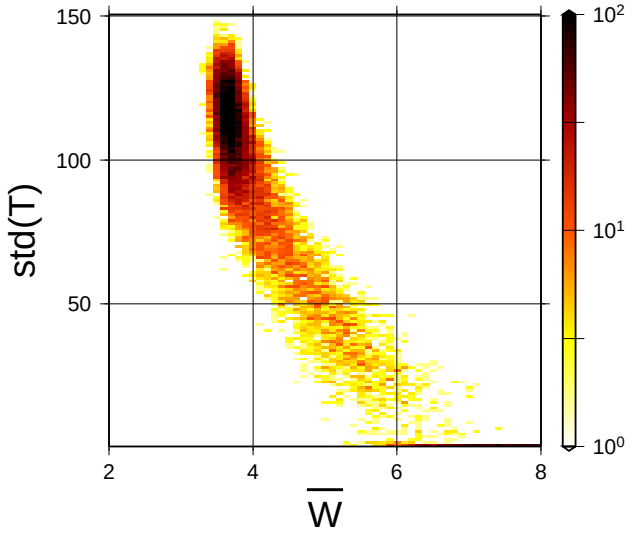

FIG. 11: (color online). The 2D histogram of links time delay variation, $STD(T_{l,r})$ and links average strength, $\overline{W}_{l,r}$. This 2D histogram is for network located at zone 1 and based on temperature measurements at 850hPa isobar.

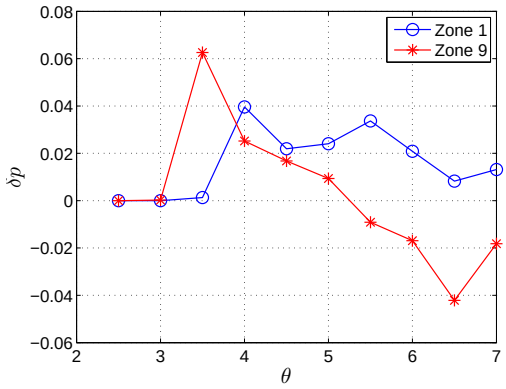

FIG. 12: (color online). The sensitivity, δp, of the stability function p as a function of the threshold θ.

value of the threshold for noise removal by the second argument θ. In Fig. 12 we show the differential of $\overline{p}(\tau;\theta)$, averaged over all values of τ, $\delta p \equiv \overline{p}(\theta+\delta\theta) - \overline{p}(\theta)$, where $\delta\theta = 0.5$. We find a sharp local maximum in δp, around $\overline{W}_{l,r} \in [3.5, 4.5]$. This sharp maximum is consistent with θ crossing the boundary between L_N and L_p, where many of the links related to noise drop off the network, and causes the average stability $\overline{p}(\theta)$ to abruptly rise. Such behavior of δp is consistent both in equatorial regions (stars) and non–equatorial regions (circles). The response of the sensitivity δp to further removal of links (which mainly belong to L_p) is thereafter reduced. In fact, removal of physical links might even result in a reduction of the stability (e.g. $\delta p < 0$), as is indeed observed for large θ in the equatorial curve in Fig. 12. In conclusion, a sharp boundary between L_N and L_p is almost certainly identified around $\overline{W}_{l,r} \approx 4.0 \pm 0.5$ in the networks calculated for all types of data (temperature and geopotential height in various altitudes covering the troposphere), both in equatorial and non–equatorial regions.

V. SUMMARY

In summary, we have established the stability of the network of connections between the dynamics of climate variables (e.g. temperatures and geopotential heights) in different geographical regions. The strength of the physical connection, $W_{l,r}$, that each link in this network represents, changes only between 5% to 30% over time. A clear boundary between links that represent real physical dependence and links that emerge due to noise is shown to exist. The distinction is based on the high link strength $W_{l,r}$ and on the variability of time delays $STD(T_{l,r})$.

Beside the stability of single links, also the hierarchy between the link strengths is preserved to a large extent. We have shown that this hierarchy is partially due to the two dimensional space in which the network is embedded, and partially due to physical coupling processes. Moreover the contribution of each of these effects, and the level of noise was explicitly estimated. The spatial effect is typically around 50% of the observed stability, and the noise reduces the stability value by typically 5%–10%.

The network structure was further shown to be consistent across different altitudes, and a monotonic relation between the altitude distance and the correspondence between the network structures is shown to exist. This yields another indication that the observed network structure represents effects of physical coupling.

The stability of the network and the contributions of different effects were summarized in specific relation to different geographical areas, and a clear distinction between equatorial and non–equatorial areas was observed. Generally, the network structure of equatorial regions is less stable and more fluctuative.

The stability and consistence of the network structure during time and across different altitudes stands in contrast to the known unstable variability of the daily anomalies of climate variables. This contrast indicates an analogy between the behavior of nodes in the climate network and the behavior of coupled chaotic oscillators [46].

A future outreach of our work can be a mapping between network features (such as network motifs) and known physical processes. Such a mapping was previously shown to exist [29] between an autonomous cluster in the climate network and El-Niño. Further structures without such a climate interpretation might point towards physical coupling processes which were not observed earlier.

[1] A.-L. Barabási and R. Albert, Science **286**, 509 (1999).
[2] A.-L. Barabaśi, *Linked: The New Science of Networks* (Perseus Publishing, 2003).
[3] M. Newman, A.-L. Barabási, and D. Watts, *The structure and dynamics of networks* (Princeton University Press, 2006).
[4] S. N. Dorogovtsev and J. F. F. Mendes, *Evolution of Networks: From Biological Nets to the Internet and WWW* (Oxford University Press, 2003).
[5] M. E. J. Newman, SIAM Review **45**, 167 (2003).
[6] D. J. Watts and S. H. Strogatz, Nature **393**, 440 (1998).
[7] I. Stewart, Nature **427**, 601 (2004).
[8] A. Barrat, M. Barthelemy, R. Pastor-Satorras, and A. Vespignani, Proc. Nat. Ac. Sc. **101**, 3747 (2004).
[9] M. Tumminello, F. Lillo, and R. N. Mantegna, Europhys. Lett. **78**, 30006 (2007).
[10] R. Albert and A.-L. Barabási, Rev. Mod. Phys. **74**, 47 (2002).
[11] R. Pastor-Satorras and A. Vespignani, *Evolution and structure of the Internet: a statistical physics approach* (Cambridge University Press, 2004).
[12] G. Caldarelli, *Scale Free Networks* (Oxford University Press, 2007).
[13] G. Caldarelli and A. Vespignani, *Large scale structure and dynamics of complex networks: from information technology to finance and natural science* (World Scientific, 2007).
[14] A. Barrat, M. Barthélemy, and A. Vespignani, *Dynamical processes on complex networks* (Cambridge University Press, 2008).
[15] M. Newman, *Networks: an introduction* (Oxford University Press, 2010).
[16] R. Cohen and S. Havlin, *Complex Networks: Structure, Robustness and Function* (Cambridge University Press, 2010).
[17] R. Albert, H. Jeong, and A.-L. Barabási, Nature **406**, 378 (2000).
[18] M. Barthélemy, Physics Reports **499**, 1 (2011).
[19] D. S. Callaway, M. E. J. Newman, S. H. Strogatz, and D. J. Watts, Phys. Rev. Lett. **85**, 5468 (2000).
[20] J. A. Acebron, L. L. Bonilla, C. J. P. Vincente, F. Ritort, and R. Spigler, Rev. Mod. Phys. **77**, 137 (2005).
[21] H. Kori and A. S. Mikhailov, Phys. Rev. Lett. **93**, 254101 (2004).
[22] R. E. Mirollo and S. H. Strogatz, SIAM J. Appl. Math **50**, 1645 (1990).
[23] B. Drossel, T. Mihaljev, and F. Greil, Phys. Rev. Lett. **94**, 088701 (2005).
[24] R. Cohen, K. Erez, D. Ben-Avraham, and S. Havlin, Phys. Rev. Lett. **85**, 4626 (2000); R. Cohen, K. Erez, D. Ben-Avraham, and S. Havlin, Phys. Rev. Lett. **86**, 3682 (2001).
[25] C. Song, S. Havlin, and H. Makse, Nature **433**, 392 (2005).
[26] I. Baruchi and E. Ben-Jacob, Phys. Rev. E **75**, 050901 (2007).
[27] K. Yamasaki, A. Gozolchiani, and S. Havlin, Phys. Rev. Lett. **100**, 228501 (2008).
[28] A. Gozolchiani, K. Yamasaki, O. Gazit, and S. Havlin, Europhys. Lett. **83**, 28005 (2008).
[29] A. Gozolchiani, S. Havlin, and K. Yamasaki, Phys. Rev. Lett. **In press** (2011).
[30] A. A. Tsonis and K. L. Swanson, Phys. Rev. Lett. **100**, 228502 (2008).
[31] J. F. Donges, Y. Zou, N. Marwan, and J. Kurths, Eur. Phys. J. Special Topics **174**, 157 (2009).
[32] J. F. Donges, Y. Zou, N. Marwan, and J. Kurths, Europhys. Lett. **87**, 48007 (2009).
[33] J. F. Donges, H. C. H. Schultz, N. Marwan, Y. Zou, and J. Kurths, arXiv (2011), 1102.3067.
[34] A. Tsonis, G. Wang, K. Swanson, F. Rodrigues, and L. Costa, Climate Dynamics **37**, 933 (2011).
[35] O. Guez, A. Gozolchiani, K. Yamasaki, Y. Berezin, S. Brenner, and S. Havlin (2011), 1109.3633, URL `http://arxiv.org/abs/1109.3633`.
[36] A. Pikovsky, M. Rosenblum, and J. Kurths, *Synchronization: A Universal Concept in Nonlinear Sciences (Cambridge Nonlinear Science Series)* (Cambridge University Press, 2003).
[37] M. Kanamitsu, W. Ebisuzaki, J. Woollen, S.-K. Yang, J. J. Hnilo, M. Fiorino, and G. L. Potter, *NCEPDOE AMIP-II Reanalysis (R-2)* (2002).
[38] E. Koscielny-Bunde, A. Bunde, S. Havlin, H. E. Roman, Y. Goldreich, and H.-J. Schellnhuber, Phys. Rev. Lett. **81**, 729 (1998).
[39] E. K. Bunde, H. E. Roman, A. Bunde, S. Havlin, and H. J. Schellnhuber, Philosophical Magazine Part B **77**, 1331 (1998).
[40] J. Pelletier and D. Turcotte, Advances in Geophysics **40**, 91 (1999).
[41] J. F. Eichner, E. Koscielny-Bunde, A. Bunde, S. Havlin, and H.-J. Schellnhuber, Phys. Rev. E **68**, 046133 (2003).
[42] A. Bunde, J. F. Eichner, J. W. Kantelhardt, and S. Havlin, Phys. Rev. Lett. **94**, 048701 (2005).
[43] M. Santhanam and H. Kantz, Physica A: Statistical Mechanics and its Applications **345**, 713 (2005).
[44] W. B. White and R. G. Peterson, Nature **380**, 699 (1996).
[45] J. Liu, X. Yuan, D. Rind, and D. G. Martinson, Geophys. Res. Lett **14**, 1679 (2002).
[46] S. Boccaletti, J. Kurths, G. Osipov, D. L. Valladares, and C. S. Zhou, Phys. Rep. **366**, 1 (2002).
[47] Similar analysis with shuffled data yields values which are smaller by typically a factor of 10
[48] When cross correlations are calculated, the continuation of the same year y is used, rather than the next random sequence
[49] The stability of the time delay with time as a criterion for a real link was proposed for physiological networks by A.Bashan R. Bartsch, J. Kantelhardt, S. Havlin, and P. Ivanov, Physiological Networks: towards systems physiology, Preprint (2011)